Mathematical Modelling of Platelet Signalling Pathways

Mark Payne

Abstract

In this dissertation we outline a mathematical model of the collagen { glycoprotein VI platelet signalling pathway. Platelets are small annucleate cell that play an important part in haemostasis. Disorders in platelet activation can be the cause of many serious disorders.

Starting from a detailed biological diagram we construct a simple schematic model of the collagen - glycoprotein VI pathway. From this model we extract the main reaction equations. Using the Law of Mass Action we change the reaction equations to a system of non-linear ordinary di erential equation which we then reduce further. After non{dimensionalising, we solve these equations numerically and nd that the model produces the desired rise in calcium within the platelet cytosol. We perform a sensitivity analysis on the model nding certain parmeters signi cantly a ect the model more than others.

We then improve the model adding IP_3 and DAG recycling as well as the

Acknowledgements

I would like to thank my supervisors Dr. Marcus Tindall and Professor Peter Grindrod as well as Dr. Mike Fry and Dr. Chris Jones for their support during writing this dissertation. I would also like to thank the ESPRC as without their funding my completion of this course would not have been possible. Lastly I would like to thank my friends Tom Holdstock and Laura Stewart for keeping me sane during my time at Reading.

Declaration

I con rm that this is my own work, and the use of all material from other sources has been properly and fully acknowledged.

Signed..... Date.....

List of Figures

Contents

Chapter 1

Introduction

The work presented in this dissertation relates to mathematically modelling chemical pathways within platelet cells. Platelets are small anucleate cells that are found within the blood, used to repair damage and stop bleeding by forming clots (thrombus). Disruption in platelet function can lead to venal thromboembolism (VTE) and other disorders. VTE is a serious condition which can lead to heart attacks or pulmonary embolism.

VTE is the blocking of a vein by the aggregation of a large number of

Figure 1.1: The thrombus formation process, from [2]

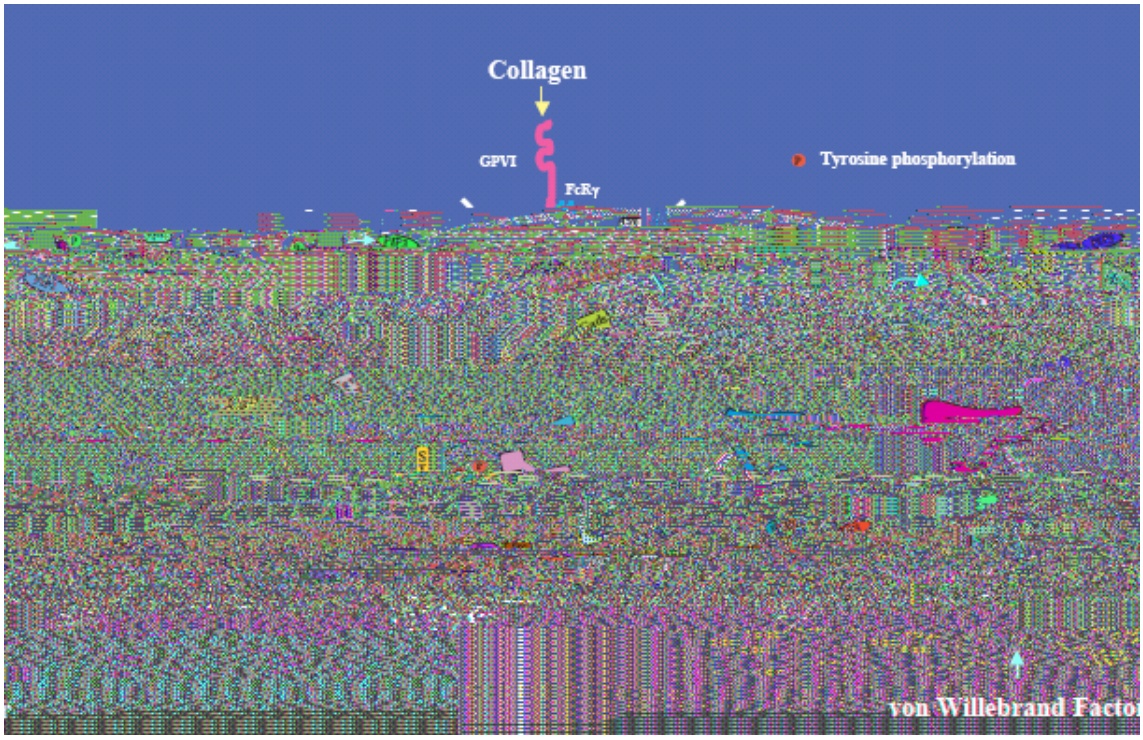

Figure 1.2: A schematic diagram indicating th collagen activated chemical pathways within the platelet, from [4]

1.1.1 Cell Signaling and the Collagen { Glycoprotein VI Receptor Signaling Pathway

Cells need to be able to react to changes in their surrounding environment and behave accordingly. To do this they use, in most cases several, chemical cascades called cell signalling pathways.

These pathways start with a receptor protein. Certain external chemicals, called receptor ligands, bind and activate these proteins. This leads to a series of internal chemical reactions that give an output such as a change in cellular behaviour or a secretion of a chemical in the extracellular space.

The chemical pathway of interest throughout this dissertation is the Collagen { Glycoprotein VI receptor (GPVI) signaling pathway. This is an important pathway as it activates at a vessel injury site.

In this pathway it is movement of calcium (Ca^{2+}) between two areas of the platelet, the dense tubular structure (DTS) and cytosol, which a ects the platelets behaviour. The pathway begins with collagen binding with GPVI, this causes the phosphorylation of SYK which in turn triggers the phosphorylation of of LAT. These interactions causes a chain of reactions that phosphorylate and activate protein further downstream which eventually leads to the transferrence of Ca^{2+} from the DTS of the platelet to it's cytosol. This leads to an increase in integrin secretion.

The mathematical modelling of cell signaling pathways within platelet cells has only been considered recently, although in other cell types it has been widely applied. The mathematical modelling of such pathways is important to help form an understanding of the a ect of any changes within the pathway, elucidating biological complexity.

The purpose of this dissertation is to develop a system of di erential equations which mathematical model the Collagen { GPVI signaling pathway. Once a suitable system has been developed we carry out analysis of

the model, such as it's sensitivity to parameter change and whether a steady state solution exists. The results of the model, the analysis and any possible further work are then discussed.

1.2 Literature Review

Mathematical models of blood coagulation mainly fall into two categories, either they focus on the chemical pathways that trigger thrombus formation or their development.

Purvis et al. [12] formulated a molecular signalling model of platelet phosphoinositide and calcium regulation during homeostatis and $P2Y_1$ activation. The network model was informed by 23 peer-reviewed studies spanning three decades of platelet research. The model consists of four distinct signalling `modules'; Ca^{2+} release and uptake, phosphoinositide metabolism, $P2Y_1$ G-protein signalling and protein kinase C regulation of phospholipase $C\{$. These four modules were then interlinked to become the full model. Non{ linear ordinary di erential equations were used to model the network modules and simulations were performed using the SBToolbox for MATLAB. The results of this model displayed similar behaviour to what was observed in experimentally. The model also ful lled the rel lled thefo e aed te fuliu1ionsthr1iosot7o8ge

thrombin generation at the sub-cellular level. The model was then used to simulate the development of a thrombus. Xu et al. [15] found that vortical flow created during the early formation of the thrombus effected it's later growth as some activated platelets were flushed back by the rolling flow to the back of the thrombus (opposing end to the direction of flow). The size of the thrombus in the simulation and it's dependence on the rate of blood flow quantitatively agreed with experimental data. The model also predicted heterogeneity within the thrombus; blood cells trapped within the thrombus, could lead to structural instability.

Pivkin et al. [11] studied the effect of blood flow velocity and the role of activation delay time on the growth and formation of thrombi. They developed a 3{D model of blood flow in a 50 m diameter straight tube, 500 m long. Several different steady blood flow rates were used and platelets were considered to be uniformly distributed in the inflow. Simulation results were compared to experimental data found previously. Pivkin and colleagues then extended the simulation to investigate the effect of the pulsatility of blood flow. They found the simulation predicted thrombi growth with shapes and patterns similar to those observed experimentally. Thrombi formed under the same flow conditions were found to have a varied time for small-growth

lation in three distinct steps; the initiation stage, the activation stage and the propagation stage. In the initiation stage a protein, tissue factor, is exposed to blood-born enzymes at the injury site which leads to small amounts of thrombin being activated. The ampli cation stage is when platelets are activated and provide a surface on which activated factors, or enzymes, to assemble and form complexes. In the propogation stage, large scale thrombin production takes place on the surface of the platelet if enough complexes are formed. A system of linked di erential equations form the model and stability analysis was carried out. Results showed that de ciencies in certain proteins within the blood reduces the rate of thrombin generation resulting in bleeding tendency which is consistent with experimental ndings.

Morbiducci et al. [9] looked at how ow patterns and stresses a ected platelet activation in mechanical heart valves. Many patients who undergo mechanical heart valve implatation sustain thromboembolic complications and thrombus deposition. The model used was one originally developed for the evaluation of mechanical damage to red blood cells but was adapted for the assessment of platelet activation state under dynamic loading conditions. The simulation was carried out with 3960 idealised platelet-like particles that were released at four di erent phases during the hearts contractions at a distance of 2mm from the valve. From the model they con rmed, through statistical analysis, that platelet activation is dependent on the phase of the cardiac cycle. They also found that the vorticity created by the valves played a role in the activation of platelets.

1.3 Outline

In this dissertation we formulate a model for the collagen{GPVI pathway. In chapter 2 we discuss the development of the model. We simplify the biological model of protein{protein intracellular reactions and identify the

reaction equations. We then form a system of ordinary di erential equations which we non-dimensionalise and then solve numerically. We then carry out sensitivity analysis of the model. The method used for our analysis is outlined and carried out. The results of our sensitivity analysis are then presented and discussed.

We extend the model more in chapter 3. The recycling of IP_3 and DAG to PI and also the movement of calcium from the cytosol to the DTS are added. This is done by adding new reaction equations which leads to a new system of di erential equations. This system is then non{dimensionalised and solved with di erences between the two models being discussed. Sensitivity analysis is then carried out and the model is tested without the presence of collagen as a check. The model is then compared to experimental data that has been supplied to us with possible reasons for di erences outlined.

In chapter 4 we draw conclusions from our work and outline future work.

Chapter 2

A Model of Platelet Signalling

In this chapter we develop a mathematical model of the Collagen { GPVI

Figure 2.1: Biological Model of the Collagen { GPVI pathway from [5].

form the inactive bound receptor, R_1, which then becomes active in (2.2). (2.3) shows the enzyme SYK then binds to the active receptor R_2 and auto-phosphorylating. The complex $SYK\ R_2$ then plays a role in the auto-phosphorylation of LAT and the phosphorylation of LAT_P in equations (2.4) and (2.5). LAT_{PP} forms a complex with $PI3K$ which then becomes active in equation (2.6). Equations (2.7), (2.8) and (2.16) form the lipid cycle. The lipid PIP_3 forms a complex with the enzyme BtK with then activates in (2.9). LAT_P and LAT_{PP} form complexes with $PLC_{\ 2}$ in (2.10) and (2.11) which then auto-phosphorylate in (2.12) and (2.13). $LAT_P\ PLC_{\ 2P}$ and $LAT_P\ PLC_{\ 2P}$ then react with PIP_2 to release IP_3 and DAG, as shown in (2.14) and (2.15). IP_3 then opens the ion channel IP_{3RO} in (2.17) to allow the calcium transfer in (2.18).

In obtaining these reaction equations we made the assumption that, for the most part, only the forward reactions played a meaningful part in the platelet pathway. This assumption is appropriate as once the platelet is activated the forward reactions must be dominant to produce the increased concentration of Ca^{2+} within the cytosol. We also assume that the proteins within the platelet are spatially homogeneous, therefore the spatial concentration of the proteins can be ignored. In our model the collagen concentration remains constant, this is due to the injury site keeps emmiting collagen and it is used by the platelet.

These reaction equations could then be transformed into a system of non-linear di erential equations using the Law of Mass Action. The Law of Mass Action [10] states that the rate of a reaction is proportional to the product of the concentration of the reactants. A source term was added to the equation for P to stop the concentration of lipids becoming zero. The system of

di erential equations, using the variables in Table 2.1, is listed below.

$$\frac{dR_0^c}{}$$

Table 2.1: Table of Variables

Notation	Meaning
C	Concentration of collagen.
R_0	Unbound GPVI receptors.
R_1	Bound, inactive GPVI receptors.
R_2	Bound, active GPVI receptors.
R_0^c	Concentration of R_0.
R_1^c	Concentration of R_1.
R_2^c	Concentration of R_2.
S	Concentration of SYK.
v_1	Concentration of the complex SYK R_2.
v_2	Concentration of the complex of phosphorylated SYK (SYK_P R_2).
L	Concentration of LAT.
L_P	Concentration of phosphorylated LAT (LAT_P).
L_{PP}	Concentration of twice phosphorylated LAT (LAT_{PP}).
P_K	Concentration of $PI3K$.
v_3	Concentration of complex of active $PI3K$ ($PI3K^*$ LAT_{PP}).
P	Concentration of PI.
P_1	Concentration of PIP.
P_2	Concentration of PIP_2.
P_3	Concentration of PIP_3.
B	Concentration of BtK.
v_4	Concentration of the complex PIP_3 BtK^*.
P	Concentration of PLC_2.
v_5	Concentration of the complex PLC_2 LAT_P.
v_6	Concentration of the complex PLC_2 LAT_{PP}.
v_7	Concentration of the complex of phosphorylated PLC_2 (PLC_{2P} LAT_P).
v_8	Concentration of the complex of PLC_{2P} LAT_{PP}.
I	Concentration of IP_3.
D	Concentration of DAG.
I_{RC}	Concentration of IP_{3RC}.
v_9	Concentration of the complex of IP_3 IP_{3RO}.
Ca_1	Concentration of calcium in the dense tubular structure ($Ca^{(1)}$).
Ca_2	Concentration of calcium in the cytosol ($Ca^{(2)}$).

Integrating we nd

$$L + L_P + L_{PP} + v_3 + v_5 + v_6 + v_7 + v_8 = \text{constant}$$

and applying the initial conditions we nd

$$L + L_P + L_{PP} + v_3 + v_5 + v_6 + v_7 + v_8 = L_T$$

where

$$L_T = L_0 + L_{P0} + L_{PP0} + v_{30} + v_{50} + v_{60} + v_{70}: \tag{2.47}$$

This means that LAT is conserved, using this we can reduce the number of parameters within the model and hence the number of equation we need to solve.

Similarly conservation of BtK (addition of equations (2.34) and (2.35)), the IP_3 receptors (addition of (2.43) and 2.44)), $PI3K$ (addition of (2.28) and (2.29)) and Ca^{2+} (addition of (2.45) and (2.46)) lead to,

$$B_T = B + v_4; \tag{2.48}$$

$$I_T = I_{RC} + v_9; \tag{2.49}$$

$$P_{KT} = P_K + v_3 \tag{2.50}$$

and

$$Ca_T = Ca_1 + Ca_2: \tag{2.51}$$

Substituting for L, v_4, P_K and Ca_1 into equations (2.26), (2.27), (2.29), (2.37)

{ (2.40) and (2.46) leads to the following reduced system of equations.

$$\frac{dR_0^c}{dt} = -k_1 R_0^c C \tag{2.52}$$

$$\frac{dR_1^c}{dt} = k_1 R_0^c C - k_2 R_1^c \tag{2.53}$$

$$\frac{dR_2^c}{dt} = k_2 R_1^c - k_3 S R_2^c \tag{2.54}$$

$$\frac{dS}{dt} = -k_3 S R_2^c \tag{2.55}$$

$$\frac{dv_1}{dt} = k_3 S R_2^c - k_4 v_1 \tag{2.56}$$

$$\frac{dv_2}{dt} = k_4 v_1 - k_6 L_P v_2 \tag{2.57}$$

$$\frac{dL_P}{dt} = k_5(L_T - L_P - L_P P - v_3 - v_5 - v_6 - v_7 - v_8)v_2 - k_6 L_P v_2 - k_{11} L_P P \tag{2.58}$$

$$\frac{dL_{PP}}{dt} = k_6 L_P v_2 - k_7 L_{PP}(P_{KT} - v_3) - k_{12} L_{PP} P \tag{2.59}$$

$$\frac{dv_3}{dt} = k_7 L_{PP}(P_{KT} - v_3) \tag{2.60}$$

$$\frac{dP}{dt} = -k_{17} P + k_{-17} P_1 + \frac{k_E}{k_s + P} \tag{2.61}$$

$$\frac{dP_1}{dt} = k_{17} P - k_{18} P_1 - k_{-17} P_1 + k_{-18} P_2 \tag{2.62}$$

$$\frac{dP_2}{dt} = -k_8 v_3 P_2 + k_9 P_3 P^{10} - k_{15} v_7 P_2 - k_{16} v_8 P_2 + k_{18} P - k_{-18} P_2 \tag{2.63}$$

$$\frac{dP_3}{dt} = k_8 v_3 P_2 - k_9 P_3 P^{10} - k_{10} P_3 B \tag{2.64}$$

$$\frac{dB}{dt} = -k_{10} P_3 B \tag{2.65}$$

k 95

$$\frac{dB_1}{dt} P \tag{2.59}$$

$$\frac{dv_5}{dt} = k_{11}L_P P \quad k_{13}(B_T \quad B)v_5 \tag{2.67}$$

$$\frac{dv_6}{dt} = k_{12}L_{PP}P \quad k_{14}(B_T \quad B)v_6 \tag{2.68}$$

$$\frac{dv_7}{dt} = k_{13}(B_T \quad B)v_5 \tag{2.69}$$

$$\frac{dv_8}{dt} = k_{14}(B_T \quad B)v_6 \tag{2.70}$$

$$\frac{dI}{dt} = k_{15}v_7P_2 + k_{16}v_8P_2 \quad k_{19}I I_{RC} \tag{2.71}$$

$$\frac{dD}{dt} = k_{15}v_7P_2 + k_{16}v_8P_2 \tag{2.72}$$

$$\frac{dI_{RC}}{dt} = \quad k_{19}I I_{RC} \tag{2.73}$$

$$\frac{dCa_2}{dt} = k_{20}(I_T \quad I_{RC})(Ca_T \quad Ca_2): \tag{2.74}$$

2.1 Parameterisation

After a literature search the initial conditions were supplied to us. Those concentrations which could not be found in the literature search were assumed to equal values of proteins who's values were known that played a similar role in the system. $PI3K$, BtK, PLC_2 and $PTEN$ are assumed to have the same concentration as SYK due to all these proteins being enzymes. LAT is assumed to have the same concentration as the receptors as it is an adaptor similar to these. We also assumed that all complexes start with zero concentration.

Reaction constants for which values could not be found were either assigned values of similar reaction constants or set relative to other parameters. k_5, k_6, k_8 { k_{16}, k_{19} and k_{20} are set relative to k_2, the parameter we will eventually non-dimensionalise with respect to. k_{-17} and k_{-18} are set relative to k_{17} and k_{18} so that the lipids PI, PIP and PIP_2 will stay constant in the absence of collagen.

Table 2.2: Values for Rate Constants

Parameter	Description	Value	Units	Reference
k_E	Source term for P	$1 \quad 10^{-11}$	$M^2 s^{-1}$	Assumed
k_s	Inhibition constant for source term	0:1	M	[8]
k_1	Rate of free receptor/collagen binding.	8:62	$(Ms)^{-1}$	[8]
k_2	Rate at which bound receptor become active.	30	s^{-1}	[3]
k_3	Rate at which SYK R_2 is formed.	325242	$(Ms)^{-1}$	[3]
k_4	Rate at which SYK_P R_2 is formed.	200	s^{-1}	[3]
k_5	Rate of LAT phosphorylation.	2469	$(Ms)^{-1}$	Assumed
k_6	Rate of LAT_P phosphorylation.	2469	$(Ms)^{-1}$	Assumed
k_7	Rate at which PI3K* LAT_{PP} is formed.	325242	$(Ms)^{-1}$	Assumed
k_8	Rate at which PIP_3 is formed.	60	$(Ms)^{-1}$	Assumed
k_9	Rate of PIP_3 converting to PIP_2.	60	$(Ms)^{-1}$	Assumed
k_{10}	Rate at which PIP_3 BtK* is formed.	60	$(Ms)^{-1}$	Assumed
k_{11}	Rate at which LAT_P PLC $_2$ is formed.	6000	$(Ms)^{-1}$	Assumed
k_{12}	Rate at which LAT_{PP} PLC $_2$ is formed.	6000	$(Ms)^{-1}$	

Table 2.3: Initial Data for concentrations

Parameter	Description	Value Used	Units	Reference
C	Collagen concentration.	$9{:}5 \quad 10^{-4}$	M	Experimental
R^c_{00}	Initial concentration of inactive, non-bound receptors.	$2{:}96 \quad 10^{-8}$	M	[13]
R^c_{10}	Initial concentration of inactive, bound receptors.	0	M	Assumed
R^c_{20}	Initial concentration of active, bound receptors.	0	M	Assumed
S_0	Initial concentration of SYK.	$9{:}865 \quad 10^{-6}$	M	[3]
v_{10}	Initial concentration of $SYK \quad R_2$.	0	M	Assumed
v_{20}	Initial concentration of $SYK_P \quad R_2$.	0	M	Assumed
L_0	Initial concentration of LAT.	$2{:}96 \quad 10^{-8}$	M	Assumed
L_{P0}	Initial concentration of LAT_P.	0	M	Assumed
L_{PP0}	Initial concentration of LAT_{PP}.	0	M	Assumed
P_{K0}	Initial concentration of PI3K.	$9{:}865 \quad 10^{-6}$	M	Assumed
v_{30}	Initial concentration of $PI3K^* \quad LAT_{PP}$.	0	M	Assumed
P_0	Initial concentration of PI.	$2{:}21 \quad 10^{-3}$	M	[12]
P_{10}	Initial concentration of PIP.	$3{:}69 \quad 10^{-4}$	M	[12]
P_{20}	Initial concentration of PIP_2.	$1{:}84 \quad 10^{-4}$	M	[12]
P_{30}	Initial concentration of PIP_3.	0	M	Assumed
B_0	Initial concentration of BtK.	$9{:}865 \quad 10^{-6}$	M	Assumed
v_{40}	Initial concentration of $PIP_3 \quad BtK^*$.	0	M	Assumed
$P_{\ 0}$	Initial concentration of PLC $_2$.	$9{:}865 \quad 10^{-6}$	M	Assumed
v_{50}	Initial concentration of $PLC_{\ 2} \quad LAT_P$.	0	M	Assumed
v_{60}	Initial concentration of $PLC_{\ 2} \quad LAT_{PP}$.	0	M	Assumed
v_{70}	Initial concentration of $PLC_{\ 2P} \quad LAT_P$.	0	M	Assumed
v_{80}	Initial concentration of $PLC_{\ 2P} \quad LAT_{PP}$.	0	M	Assumed
I_0	Initial concentration of IP_3.	0	M	Assumed
D_0	Initial concentration of DAG.	0	M	Assumed
I_{RC0}	Initial concentration of IP_{3RC}.	$4{:}61 \quad 10^{-7}$	M	[12]
v_{90}	Initial concentration of $IP_3 \quad IP_{3RO}$.	0	M	Assumed
Ca_{10}	Initial concentration of Calcium in the DTS.	$5 \quad 10^{-3}$	M	[12]
Ca_{20}	Initial concentration of Calcium in the Cytosol.	$50 \quad 10^{-9}$	M	[12]
P_0^{10}	Initial concentration of PTEN.	$9{:}865 \quad 10^{-6}$	M	Assumed

2.2 Non{Dimensionalisation

Before solving our model we decided to non{dimensionalise the equations above. Non{dimensionalising removes the dimensions of the parameters so they can be directly compared and the reduces the number of parameters. We non{dimensional variable with respect to k_2 so

$$t = \frac{}{k_2}; \tag{2.75}$$

where is the non-dimensional variable. We further more assume that all the concentrations are scaled with respect to Ca_T. So, for example

$$C = Ca_T\bar{C}; \tag{2.76}$$

where $\bar{C}$ is the non-dimensional concentration.

The system of equations then becomes

$$\frac{dR_0^{cc}}{d} = k_1R_0^{cc}\bar{C} \tag{2.77}$$

$$\frac{dR_1^{cc}}{d} = k_1R_0^{cc}\bar{C} \quad k_2R_1^{cc} \tag{2.78}$$

$$\frac{dR_2^{cc}}{d} = k_2R_1^{cc} \quad k_3\bar{S}R_2^{cc} \tag{2.79}$$

$$\frac{d\bar{S}}{d} = k_3\bar{S}R_2^{cc} \tag{2.80}$$

$$\frac{d\bar{v}_1}{d} = k_3\bar{S}R_2^{cc} \quad k_4\bar{v}_1 \tag{2.81}$$

$$\frac{d\bar{v}_2}{d} = k_4\bar{v}_1 \quad k_6L_P^{c}\bar{v}_2 \tag{2.82}$$

$$\frac{dL_P^{c}}{d} = k_5(L_T^{c} \quad L_P^{c} \quad L_P^{d} \quad \bar{v}_3 \quad \bar{v}_5 \quad \bar{v}_6 \quad \bar{v}_7 \quad \bar{v}_8v_1 \quad k_3L^{c}\bar{v}$$

$$\frac{dL\Phi_P}{d} = k_6 L\Phi_P \Psi_2 \quad k_7 L\Phi_P (P\Phi_{KT} \quad \Psi_3)$$

where

$$k_E = \frac{k_E}{k_2 Ca_T^2};\ k_s = \frac{k_s}{Ca_T}; \tag{2.100}$$

$$k_1 = \frac{k_1 Ca_T}{k_2};\ k_3 = \frac{k_3 Ca_T}{k_2};\ k_4 = \frac{k_4}{k_2}; \tag{2.101}$$

$$; \quad _T$$

(2.1062

Parameter	Description	Value
k_E	Source term for PI	$1{:}3 \quad 10^{-6}$
k_s	Inhibition constant for source term	20
k_1	Rate of free receptor/collagen binding.	0:0014
k_2	Rate at which bound receptor become active.	1
k_3	Rate at which SYK R_2 is formed.	54:21
k_4	Rate at which SYK_P R_2 is formed.	6:67
k_5	Rate of LAT phosphorylation.	0:41
k_6	Rate of LAT_P phosphorylation.	0:41
k_7	Rate at which $PI3K^*$ LAT_{PP} is formed.	54:21
k_8	Rate at which PIP_3 is formed.	0:01
k_9	Rate of PIP_3 converting to PIP_2.	0:01
k_{10}	Rate at which PIP_3 BtK^* is formed.	0:01
k_{11}	Rate at which LAT_P PLC $_2$ is formed.	

Parameter	Description	Value
θ	Collagen concentration.	0:19
R_{00}^{inact}	Initial concentration of inactive, non-bound receptors.	$5{:}92 \quad 10^{-6}$
R_{10}^{inact}	Initial concentration of inactive, bound receptors.	0
R_{20}^{act}	Initial concentration of active, bound receptors.	0
S_0	Initial concentration of SYK.	0:002
v_{40}	Initial concentration of $SYK \quad R_2$.	0

refer to [7].

2.3.1 Backwards Di erentiation

The backward di erentiation formula are a set of implicit methods that can be used to numerically solve di erential equations. They are linear multistep methods that approximate the derivative of the function using data that has been calculated at previous timesteps.

The general form of a linear multistep method to solve the di erential equation

$$\underline{y}' = \underline{f}(t; \underline{y}); \ \underline{y}(t_0) = y_0$$

is

$$\sum_{i=0}^{k} a_i \underline{y}_{n-i} = h \sum_{i=0}^{k} b_i \underline{f}_{n-i}.$$

Backwards di erentiation methods have $b_i = 0$ for $i > 0$ and so the general formula becomes

$$\sum_{i=0}^{k} a_i \underline{y}_{n-i} =$$

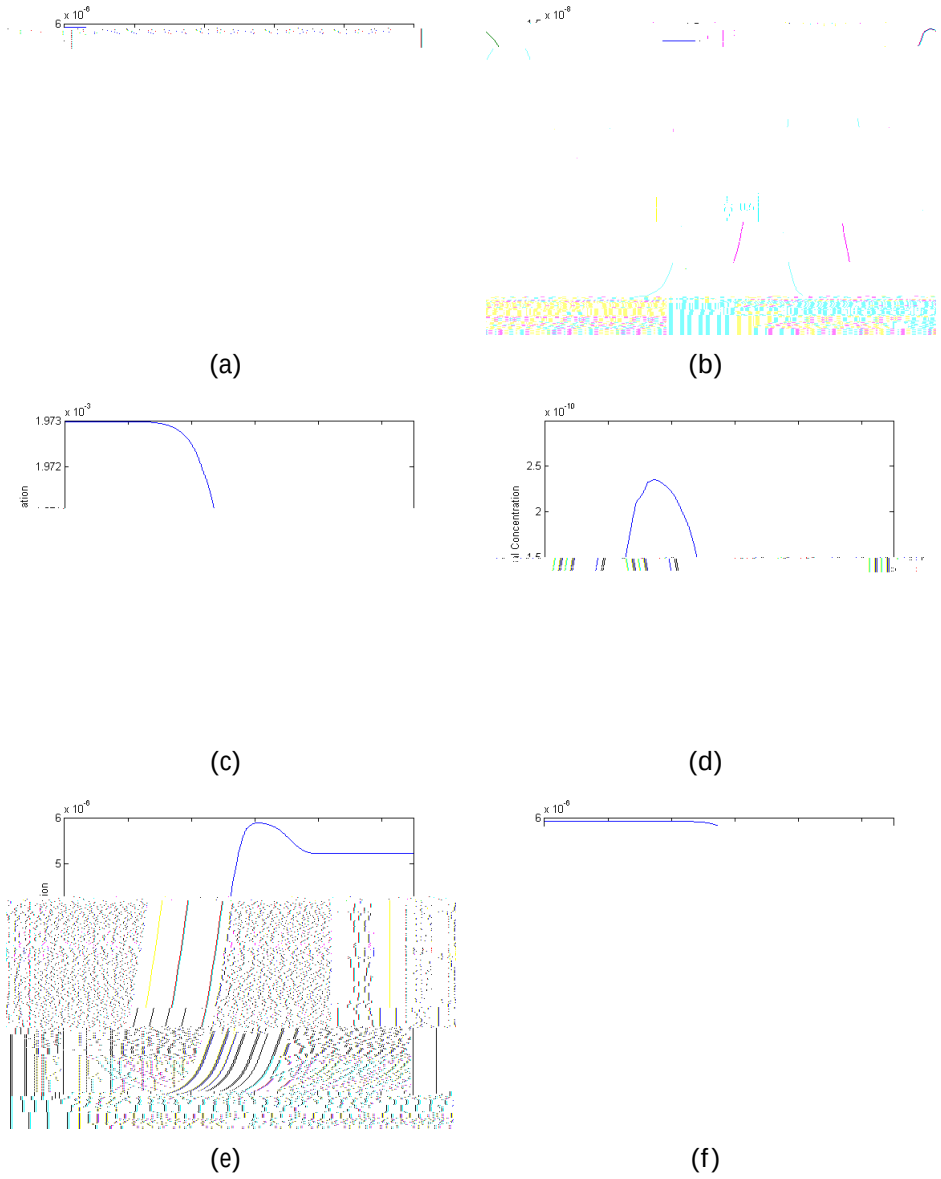

Figure 2.3: Graphs of Non{Dimensional Concentration against Time in seconds. (a)R_0, (b)R_1 and R_2, (c)SYK, (d)$SYK\ R_2$, (e)$SYK_P\ R_2$ and (f)LAT.

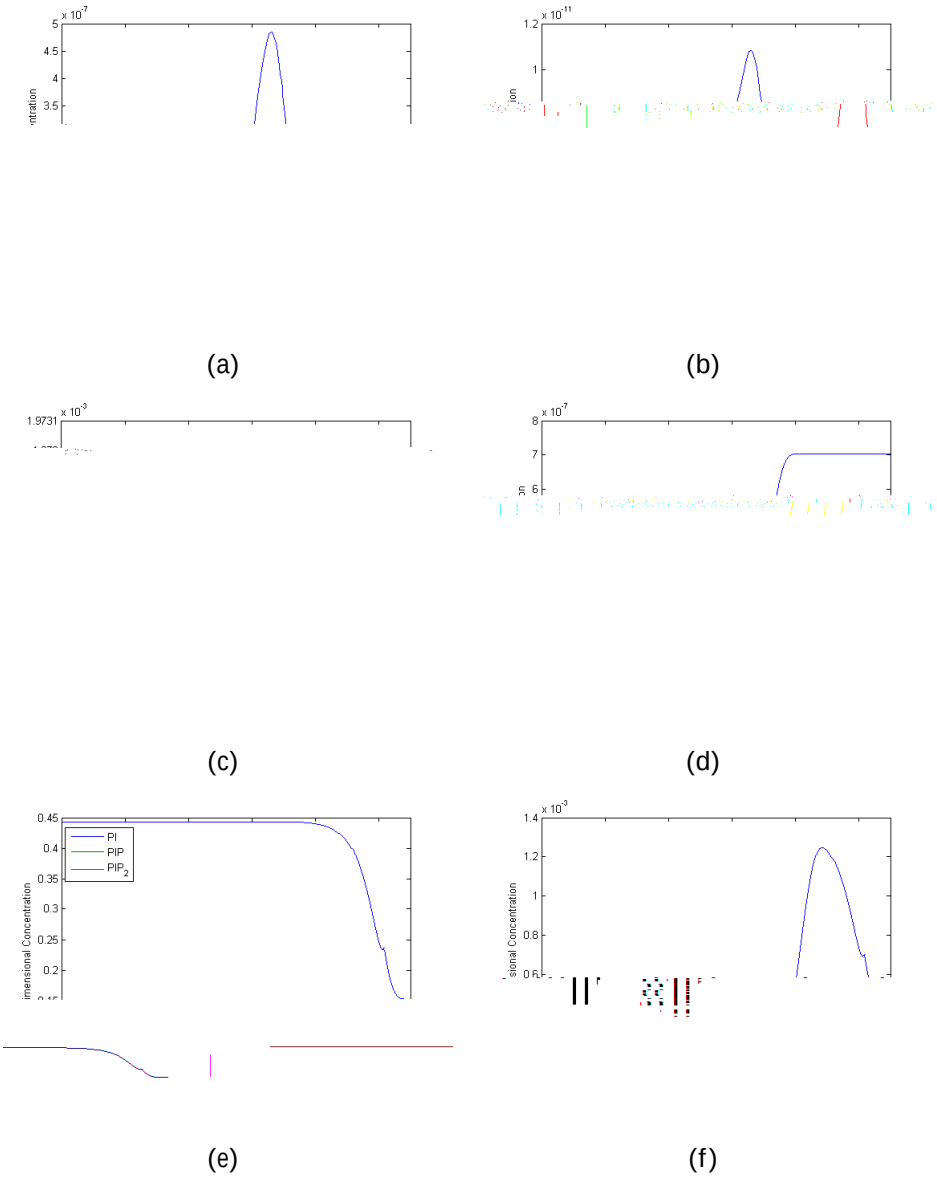

Figure 2.4: Graphs of Non{Dimensional Concentration against Time in seconds. (a)LAT_P, (b)LATLAT

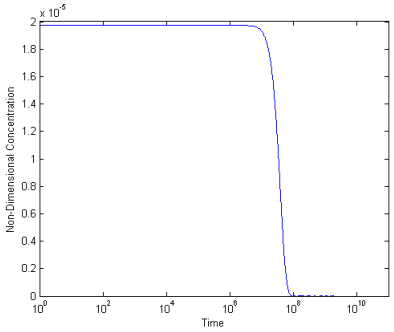
x 10^-5
2
1.8
1.6
1.4
1.2
1
0.8
0.6
0.4
0.2
0
Non-Dimensional Concentration
10^0
10^2
10^4
10^6
10^8
10^10
Time

(a)

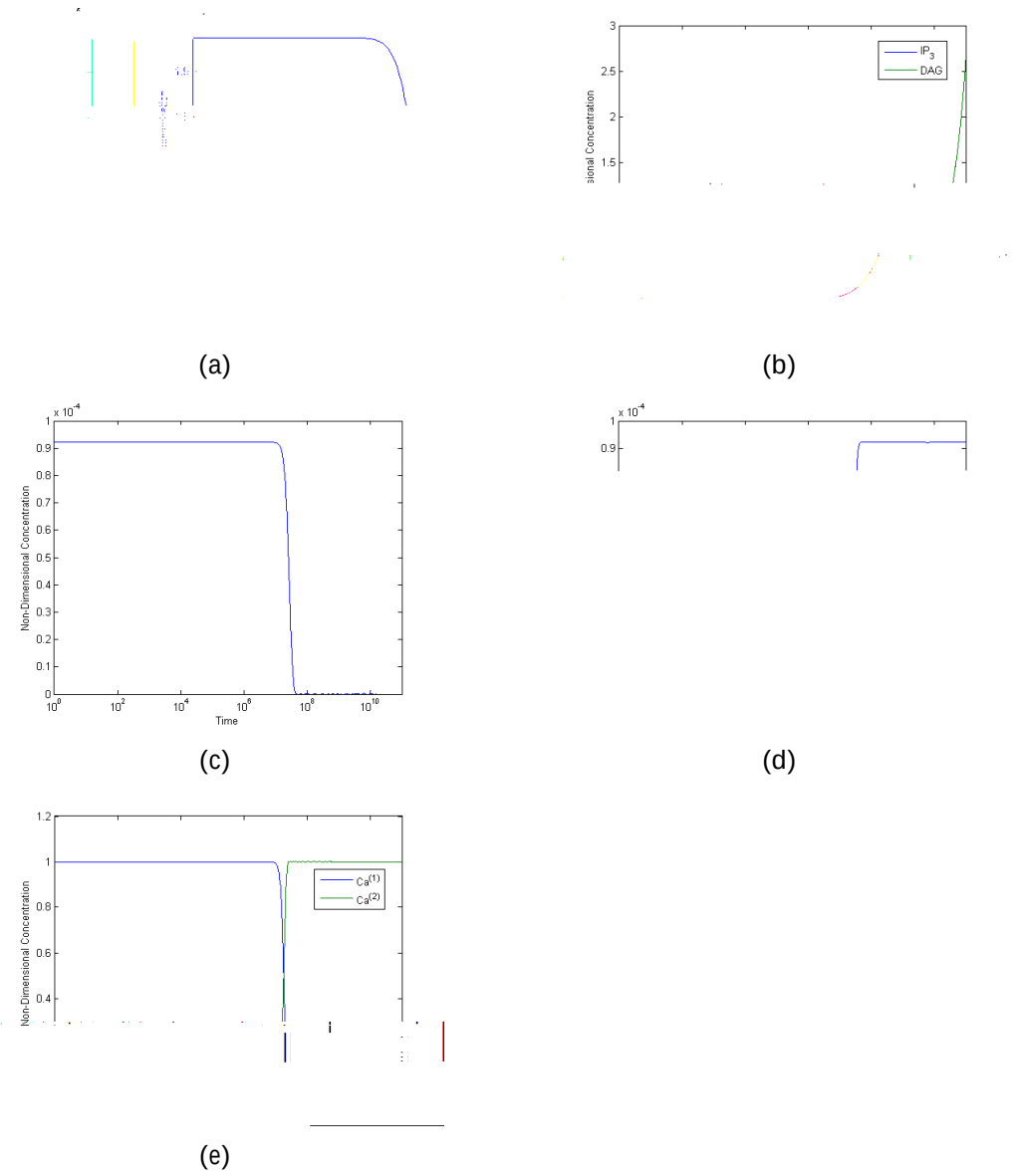

(a) (b)

(c) (d)

(e)

Figure 2.6: Graphs of Non{Dimensional Concentration against Time in seconds. (a)PLC_2, (b)IP_3 and DAG, (c)IP_{3RC}, (d)IP_3 IP_{3RO}, (e)$Ca^{(1)}$ and $Ca^{(2)}$.

2.4 Model Solutions

Figures (2.3) { (2.6) are the numerical solution to the system of di erential equations described in the previous section. They show the change in concentration of the proteins involved in the pathway described in Figure (2.2). Figure (2.3) shows the concentrations of proteins at the beginning of the pathway . We can see how quickly the collagen binds to the receptor and the receptors become active, this is due to collagen being in excess. SYK then binds with these active receptors, reducing it's concentration, and auto-phosphorylates. This phosphorylated complex then is used in the auto{phosphorylation of LAT, producing LAT_P and being used up when generating LAT_{PP}.

In Figure (2.4) we see LAT_{PP} being used to activate $PI3K$ by forming the complex LAT_{PP} $PI3K$. The lipids PI, PIP and PIP_2 slowly arrive at a steady state with PIP_3 rising as it's generated then reducing as the reaction

driving the reaction (2.1) and (2.2) combined with the fast reaction rates in reaction (2.3). This means that R_1 and R_2 are used almost as fast as they are generated. Similarly, this is the case for only small increases LAT_P, LAT_{PP} and $LAT_{PP}\ PLC_2$ before their reduction. $PI3K^*\ LAT_{PP}$ and $LAT_{PP}\ PLC_2$ settle to small concentration, this is due to LAT, of one form or another being involved in many of the reactions and so the initial concentration of LAT being split.

2.5 Sensitivity Analysis of the Model

varied each parameter and used several features of the results (rst, second and third oscillations) of their model to quantify the e ect on the outcome.

We, however, do not have enough features on our graphs to make this method work e ectively. So the method which we will use to analyse our model, is to vary each parameter in the model individually and then merely look at the e ect on one key feature of the model. We times each parameter by 10, 50, 100, 0:1, 0:05 and 0:01 while keeping the rest at their original value. We measure the time it took for Ca_2 to be higher that Ca_1 and compare it to the model with original values.

2.5.2 Analysis and Discussion

Unfortunately numerical problems meant we could not run a sensitivity analysis for IP_3 or BtK initial concentration. However all other non-zero concentrations were taken into account.

Looking at gure (2.7) we can see that changes in k_{20} have a large a ect on the output. This is expected as k_{20} is the rate of transfer between calcium in the DTS and cytosol. Similarly the a ect of k_{19} could be predicted as it opens the ion channel so transferrence can take place. The rate constants k_{17}, k_{-17}, k_{18} and k_{-18} which control lipid cycling can also be seen to be important. This could be as PIP_2 is needed to generate IP_3, so the more PIP_2 in the system the more IP_3 is produced, which is needed to release calcium from the DTS. The need for IP_3 in the system is also backed up by the a ect of varying k_{15}. It is possible that a greater amount of IP_3 is produced from LAT_P PLC_{2P} than from LAT_{PP} PLC_{2P} which is why it has more of an a ect on the output. It can be seen reduction in k_5 lengthens the time it takes for calcium to be released. From Figure (2.2) we see that the model branches into two after LAT_P is produced, k_5 is at the junction of this branching and so has a greater a ect on the model output as LAT_P avaliability will contribute to many reaction downstream indirectly.

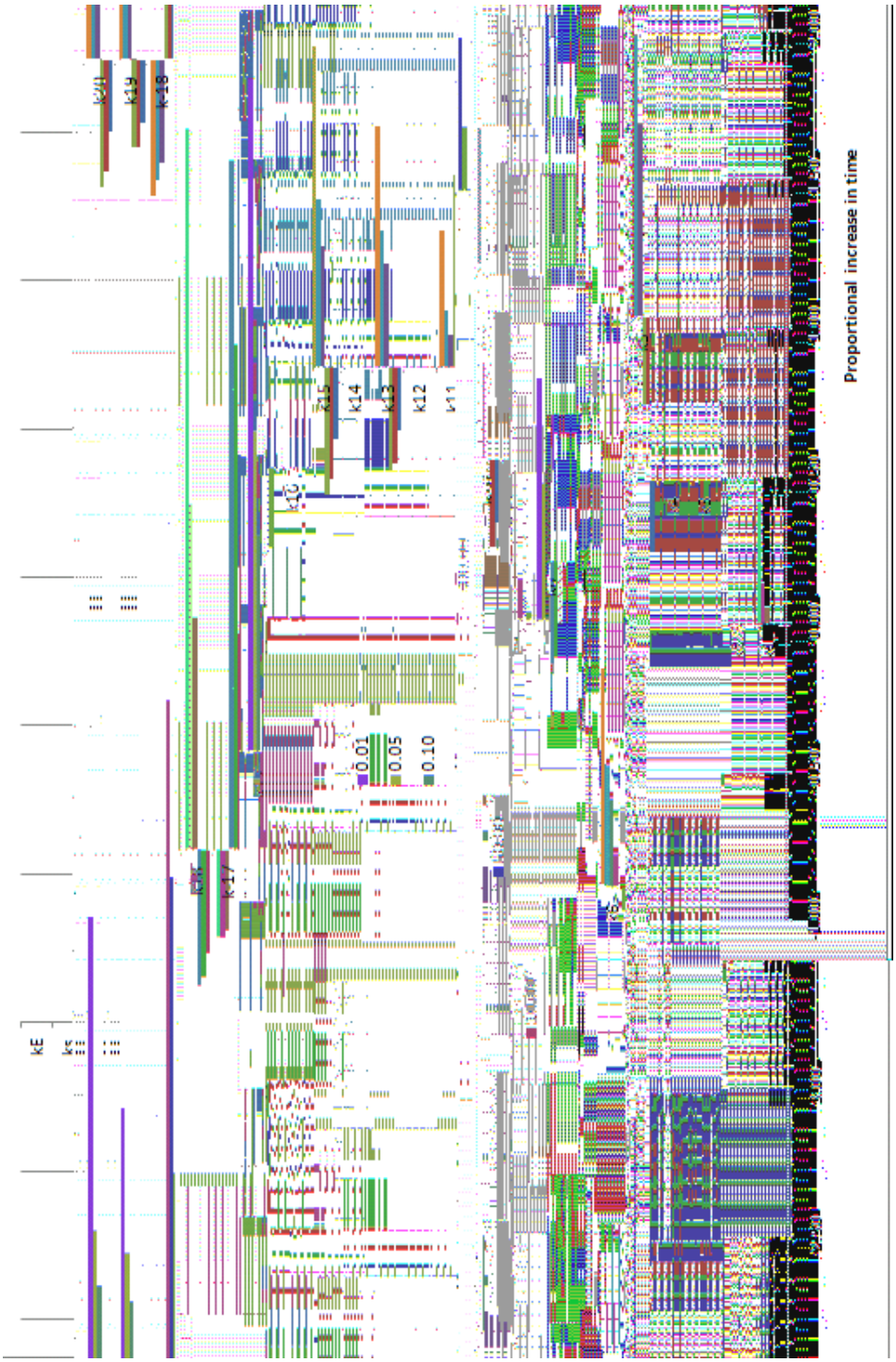

Figure 2.7: Graph showing a ect of changing rate constants on model output

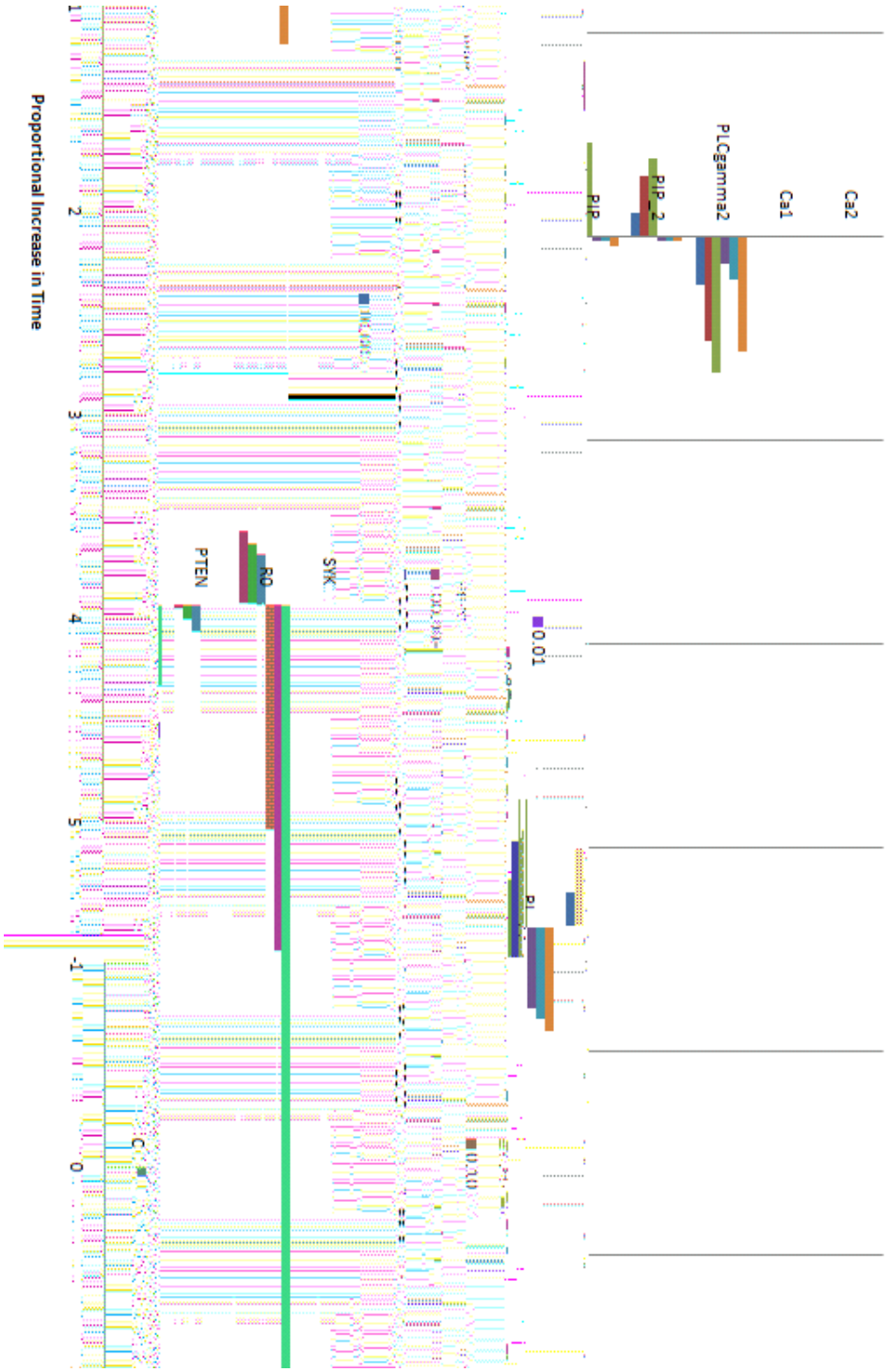

Figure 2.8: Graph showing a ect of changing initial concentrations on model output

The next most in uential rates are k_6, k_8, k_{10} and k_{13}. The rst three of these rates lie on the same branch of the model. It is this branch eventually generates PIP_3 BtK^*, which is necessary to produce LAT_P PLC_{2P} and LAT_{PP} PLC_{2P} which are needed for IP_3 generation. k_{13} is the rate that controls the formation of LAT_P PLC_{2P}, which preceeds the reaction which k_{15} controls, so is in uential for a similar reason. An increase or decrease in k_{11} increases the time it takes for the transfer of calcium. This could be because it regulates the rate at which LAT_P is used to form LAT_P PLC_2

time. PLC_2 slows the time it takes for calcium transfer if it is increased or decreased. This could be because if the concentration is high, it reacts with more LAT_{PP} taking it away from the branch which produces PIP_3 BtK^* which is important as stated before. If there is low concentration not enough LAT_P PLC_2 will be produced on the branch that produces the greater amount of IP_3:

Chapter 3

Improving the Model

Although the model transfers calcium from the DTS to the cytosol as required, however there are some problems. The fact that IP_3 and DAG never reach a steady state, and that the DTS empties of calcium completely is intuitively wrong. Now we try and adapt the model to make it more realistic. We add the recycling of IP_3 and DAG aswell of the recycling of calcium in the cytosol to the DTS. Changes to our model can be seen in Figure (3.1). We add the following two reaction equations,

$$IP_3 + DAG \xrightarrow{k_{21}} PI \tag{3.1}$$

$$Ca^{(2)} + SERCA \xrightarrow{k_{22}} Ca^{(1)} + SERCA \tag{3.2}$$

and so equations (2.61), (2.71), (2.72) and (2.74) now become

$$\frac{dP}{dt} = k_{17}P + k_{-17}P_1 + k_{21}DI \tag{3.3}$$

$$\frac{dI}{dt} = k_{15}v_7P_2 + k$$

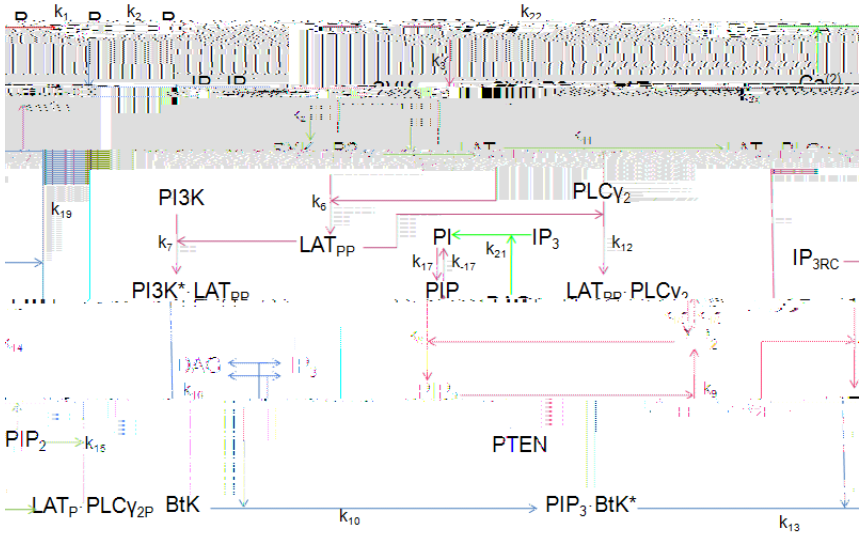

Figure 3.1: Schematic Diagram of improved Model. Changes are shown in red.

$$\frac{dD}{dt} = k_{15}v_7P_2 + k_{16}v_8P_2 \quad k_{21}DI \tag{3.6}$$

$$\frac{dCa_2}{dt} = k_{20}(I_T \quad I_{RC})(Ca_T \quad Ca_2) \quad k_{22}Ca_2S^A: \tag{3.7}$$

and we assume the initial concentration of $SERCA$ to be $S_0^A = 9{:}865$ $10^{-6}M$, the same as P^{10}. We also a252 0

$$\frac{dP}{d\tau} = k_{15}\phi_T P_2 + k_{16}\phi_B P_2 - k_{19} P I_{RC} - k_{21} D P \tag{3.9}$$

$$\frac{dD}{d\tau} = k_{15}\phi_T P_2 + k_{16}\phi_B P_2 - k_{21} D P \tag{3.10}$$

$$\frac{dCa_2}{d\tau} = k_{20}(I_T - I_{RC})(Ca_T - Ca_2) - k_{22} Ca_2 S^{CA} \tag{3.11}$$

with

$$k_{21} = \frac{k_{21} Ca_T}{k_2};\ k_{22} = \frac{k_{22} Ca_T}{k_2}$$

and the other non-dimensional parameters as before. Hence we have S_0^{CA} =

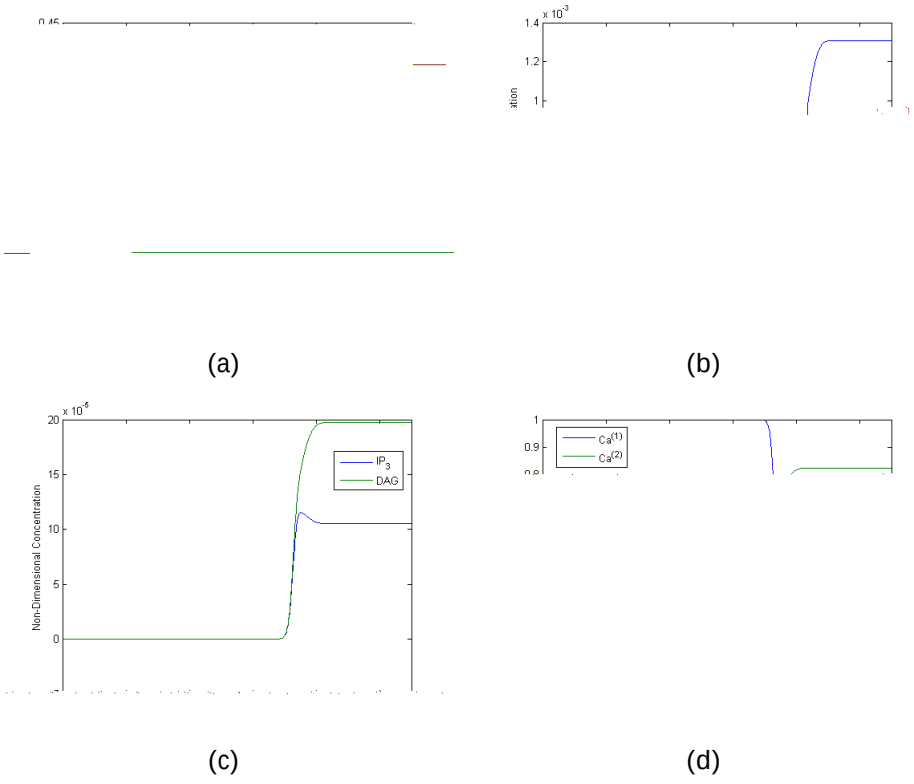

Figure 3.2: Graphs for the Improved Model. (a)PI, PIP and PIP_2, (b) PIP_3, (c) IP_3 and DAG (d) $Ca^{(1)}$ and $Ca^{(2)}$.

k_{19} to give a better idea of scale.

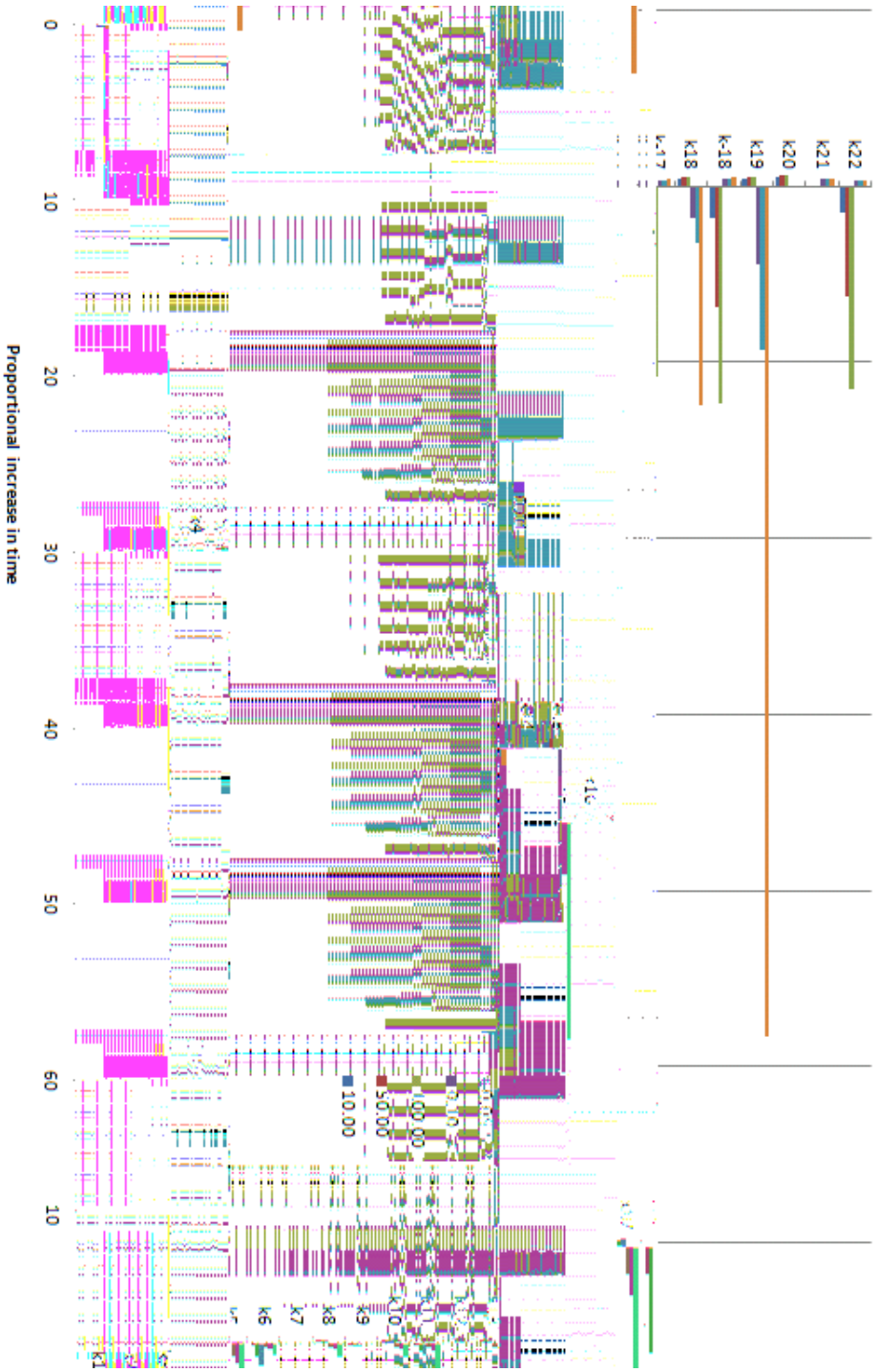

Figure 3.3: Graph showing a ect of changing rate constants on model output

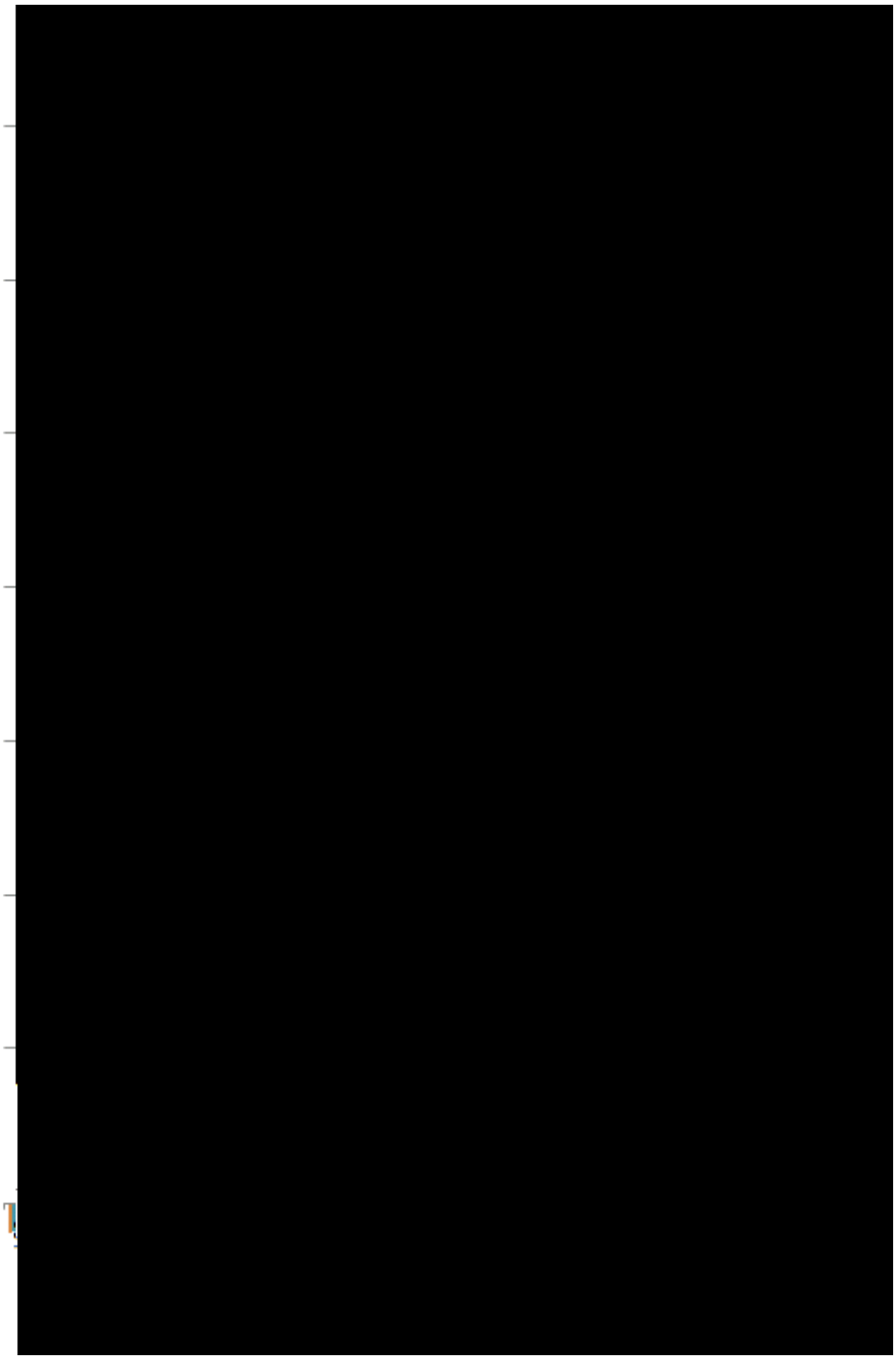

Figure 3.4: Graph showing a ect of changing rate constants on model output, with k_{19} removed

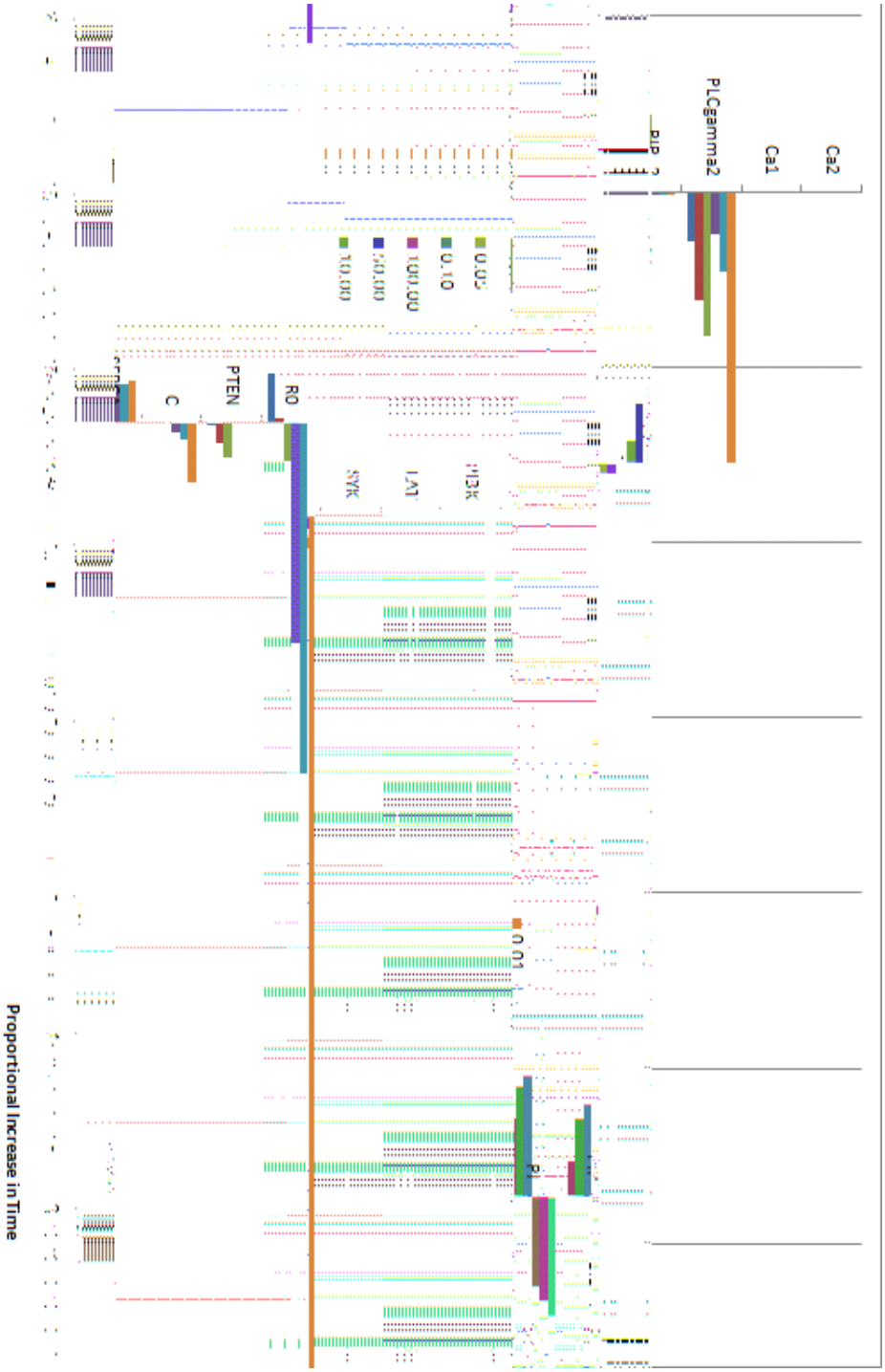

Figure 3.5: Graph showing a ect of changing initial concentrations on model output

the system of equations

$$0 = k_{17}[b] + k_{-17}[c_1] + k_{21}[D][b] \tag{3.12}$$

$$0 = k_{17}[b] - k_{18}[c_1] - k_{-17}[c_1] + k_{-18}[c_2] \tag{3.13}$$

$$0 = k_8\theta_8[c_2] + k_9[c_3][d]_0 - k_{15}\theta_7[c_2] - k_{16}\theta_8[c_2] + k_{18}[c_1] - k_{-18}[c_2] \tag{3.14}$$

$$0 = k_8\theta_8[c_2] - k_9[c_3][d]_0 \tag{3.15}$$

$$0 = k_{15}\theta_7[c_2] + k_{16}\theta_8[c_2] - k_{21}[D][b] \tag{3.16}$$

$$0 = k_{20}([b]_T - I_{RC})([a]_T - [a]_2) - k_{22}[a]_2[S]_A \tag{3.17}$$

to solve.

We can see from numerical results that $I_{RC} = 0$ at steady state, which means from equation (3.17) we find

$$[a]_2 = \frac{k_{20}[b]_T[a]_T}{k_{20}[b]_T + k_{22}[S]_A} \tag{3.18}$$

with the equations (3.12) – (3.16) giving us the relations

$$[b] = \frac{(k_{-17} + k_18)[c_1] + k_{-18}[c_2]}{k_{17}} \tag{3.19}$$

$$[D] = \frac{k_{18}[c_1] + k_{-18}[c_2]}{k_{21}[b]} \tag{3.20}$$

$$\theta_8 = \frac{k_9[c_3][d]_0}{k_8[c_2]} \tag{3.21}$$

$$\theta_7 = \frac{(k_{18} - k_{16}\theta_8)[c_2] + k_{18}[c_1]}{k_{15}[c_2]}$$

amount of variables involved. We could approximate the steady state of the lipids PI, PIP and PIP_2 by their initial concentrations as it can be seen from Figure (3.2) their steady states di er little from this. This would reduce the number of variables an may give us more useful relations.

3.5 Comparison to Experimental Data

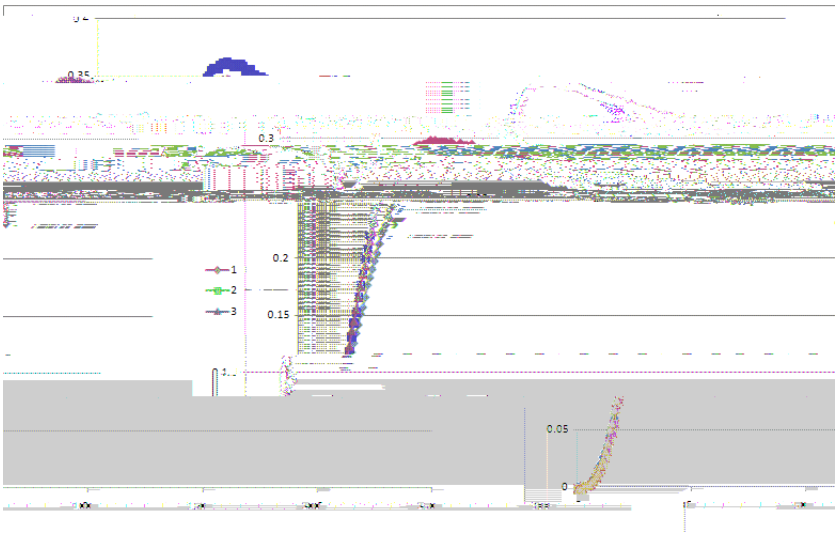

(a)

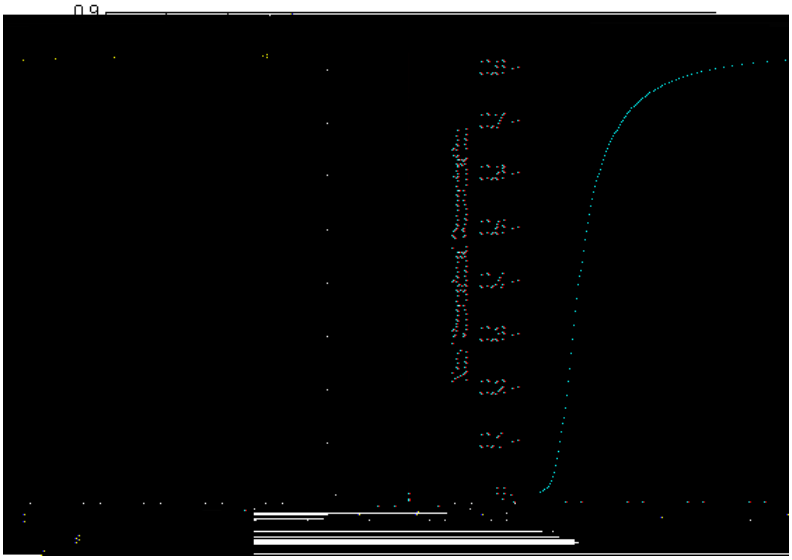

(b)

Figure 3.6: Graphs showing (a) experimental calcium in cytosol over time and (b) model calcium in cytosol over time.

Chapter 4

Conclusions and Discussion

This dissertation has formulated and solved a model for the collagen{GPVI pathway. We found the model transfers calcium from the DTS to the cytosol as required. We carried out a sensitivity analysis of this model finding k_{20}, which is the rate directly effecting calcium transfer to have a great influence. In addition we found concentrations and rate constants connected to the lipid cycle being influential in the model as well as k_5, the rate constant before Figure (2.2) can be seen to branch in two.

The first model, however, had some problems. It emptied the DTS of calcium, as well as having the problem of IP_3 and DAG not reaching steady states. An improved model was formulated, including the recycling of IP_3 and DAG into PI and the movement of calcium back into the DTS. Sensitivity analysis of this model found very similar influential parameters to that of the first model. However k_{22} now becomes less significant, the concentration of $SERCA$ as well as the rate constant k_{22} have a more than average affect on the model.

Comparing to experimental data we find that although calcium in the cytosol rises in our model, it takes much longer. We also find that the behaviour of our calcium level doesn't match the experimental data which

exhibits a rise and a small fall.

The technique we used to form our model was one which modelled the whole pathway at once. Another way would have been to separate the pathway into module, as in [12]. The advantages this would have given us is that we could more accurately study each part of the pathway, and the a ect of parameter changes within the modules. The problem may have been tting the pathway together after this as though a enclosed module may work well enough on its own, it may not work in the context of the whole pathway once connected with others.

4.1 Future Work

Our model only considers forward reactions, although all the reactions in our model are reversible. The inclusion of backward reactions in our model may produce a more realistic calcium behaviour. We could also include inhibition as in [12].

The majority of the parameters within our model have been assumed. To make the model work more accurately it would be advisable to do a literature search to nd reliable values for all rate constants and initial concentrations.

Extension of the pathway may also be possible. We may wish to add other parts of the pathway featured in Figure (2.1) or possibly some of the modules in [12]. We could also increase the pathway past calcium to include secretion of thrombin.

We also assumed in this model that the platelet is spatially heterogeneous. This is not the case in actual platelets, this means we could add to our model a spatial aspect. This would mean using partial di erential equations as

Bibliography

[1] American Heart Association. Venous thromboembolism and pulmonary embolism { statisitics. www.americanheart.org/downloadable/heart/1200598191688FS29VTE08.pdf.

[2] Barrett, N., Holbrook, L., Jones, S., Kaiser, W., Moraes, L., Rana, R., Sage, T., Stanley, R., Tucker, K., Wright, B., and Gibbins, J. Future innovations in anti-platelet therapies. *Br. J. Pharmacol. 154* (2008), 918{939.

[3] Faeder, J., Hlavacek, W., Reischl, I., Blinov, M., Metzger, H., Redondo, A., Wofsy, C., and Goldstein, B. Investigation of early events in fc ri{mediated signaling using a detailed mathematical *rifmeJ0(154)]Imm*

nalling in the nf- b: the roles of ikk and i b . *Sys. Biol. 1*

[15] Xu, Z., Chen, N., Kamocka, M., Rosen, E., and Alber, M. A multiscale model of thrombus development. *J. R. Soc. Interface 5* (2008), 705{722.